

# Low temperature Magneto-dielectric coupling in nanoscale layered $\text{SmFe}_{0.5}\text{Co}_{0.5}\text{O}_3$ perovskite

Ashish Shukla<sup>1</sup>, Akash Singh<sup>1</sup>, Md. Motin Seikh<sup>2</sup> and Asish K Kundu<sup>1\*</sup>

<sup>1</sup>*Discipline of Physics, Indian Institute of Information Technology, Design & Manufacturing Jabalpur, Dumna*

*Airport Road, Madhya Pradesh-482005, India*

<sup>2</sup>*Department of Chemistry, Visva-Bharati, Santiniketan, West Bengal -731235, India*

## Abstract

We have carried out different physical characterization by magnetic and dielectric measurements on nanoscale layered mixed Fe-Co layers orthoferrite  $\text{SmFe}_{0.5}\text{Co}_{0.5}\text{O}_3$ . The magnetization results reveal that the system is antiferromagnetic with a magnetic transition around 310 K and two spin-reorientation transitions at around 192 K and 22 K respectively. In this phase, the antisymmetric exchange interaction induces weak ferromagnetism due to a canting of the magnetic spins akin to Ln-Fe-Co system. Importantly, this nanoscale layered perovskite also shows positive magneto-dielectric effect of around 2.5% (100 K) and the value decreases on both side of this temperature. We have analyzed the conditions for the existence of magnetic and dielectric coupling in terms of the magnetic interactions between the cations along with the spin-lattice interactions in low temperature range.

*Keywords:* Orthoferrites; Ferromagnetic; Antiferromagnetic; Dzyaloshinskii-Moriya interaction; Dielectric constant

---

\*Corresponding author e-mail: [asish.k@gmail.com](mailto:asish.k@gmail.com)/[asish.kundu@iitdmj.ac.in](mailto:asish.kundu@iitdmj.ac.in)

## 1. Introduction

Perovskite based multiferroics materials have attracted enduring attention because of the wide variety of physical properties [1-5]. Designing of multiferroics is a challenging issue in transition metal perovskites. The prevalence of conjugate ordering in magnetic and electric parameters is of paramount importance from the view point of next generation magneto-electric devices. These interesting physical properties prompted researchers to design numerous novel devices. In the past few years, materials such as perovskite lanthanide ferrites  $\text{LnFeO}_3$  have been of fundamental interest owing to their potential applications for ultrafast lasers in magnetic devices, and also promising materials for multiferroics [6-10]. In these orthoferrites the  $\text{Fe}^{3+}$  ions form two magnetic sublattices, the spins of which are antiferromagnetically coupled. Also, the coupling of electronic orbital states to ordered spins determine the magnetic anisotropy in magneto-electric and multiferroic materials. Additionally, the basic understanding of magnetic interactions between the lanthanide  $\text{Ln}^{3+}$ - $4f$  and transition metal  $\text{Fe}^{3+}$ - $3d$  is a very challenging topic that has been influencing their physical properties immensely, as proven for  $\text{NdFeO}_3$  [11]. Likewise, in perovskite  $\text{ErFeO}_3$  the magnetic phase transition can be explicitly explained by  $\text{Fe}^{3+}(3d)$ - $\text{Er}^{3+}(4f)$  exchange coupling constants [10]. Interestingly, the  $\text{SmFeO}_3$  compound is also a class of orthoferrites and that has been investigated recently by several groups for its controversial multiferroic properties [12-15]. Lee et al [12] have reported  $\text{SmFeO}_3$  compound by means of theoretical and experimental evidences, which possess improper ferroelectricity at room temperature and magnetization reversal at low temperature. However, the existence of ferroelectricity has been denied for  $\text{SmFeO}_3$  considering various experimental investigations by Kuo et al [15], and suggested that the magneto-elastic effects lead to an artificial ferroelectricity.

Based on these results we have understood that the origin of ambiguous ferroelectricity in  $\text{SmFeO}_3$  may be due to different synthesis conditions, which in turn are related to the different lossy character of the samples [12,15]. Moreover, it has been observed that the multiferroic and magneto-dielectric behavior in B-site doped ferrites  $\text{LnFeO}_3$  could be achieved by using different transition metals [16,17]. Therefore, in this paper we have focused on two parameters, first, the B-site doping in  $\text{SmFeO}_3$  i.e. 50 % iron is replaced by cobalt and secondly, we adopted the sol-gel synthesis process, which certainly has many advantages when compared with other techniques [18]. One of the most important advantage of this technique being the possibility of controlling the chemical reaction at molecular level resulting in better crystallinity and phase formation. Present nanoscale layered  $\text{SmFe}_{0.5}\text{Co}_{0.5}\text{O}_3$  perovskite crystallizes in orthorhombic structure (space group: Pnma), akin to parent  $\text{SmFeO}_3$  [12-15] and  $\text{SmCoO}_3$  [19,20] phases. Recently, we have reported that this perovskite exhibits a unique nanostructure built up of mixed Fe-Co octahedral layers involving a gradual and periodic variation of the cations from Co-rich to Fe-rich layers [21]. Considering the ability of Fe/Co cations to occupy the same B-site in the perovskite  $\text{ABO}_3$ , the design of mixed Fe-Co perovskite offers a wide field for the realization of interesting magnetic and dielectric properties. Herein, we report the results of unusual and complex magnetic transition of the nanoscale layered  $\text{SmFe}_{0.5}\text{Co}_{0.5}\text{O}_3$  phase, an important feature of antiferromagnetism which is the anomalously small ordered moment for  $\text{Fe}^{3+}$  and  $\text{Co}^{3+}$ , similar to its parent phases [12,19-21]. Moreover, this nanoscale layered  $\text{SmFe}_{0.5}\text{Co}_{0.5}\text{O}_3$  phase exhibits positive magneto-dielectric effect of 2.5 % at low temperature (100 K) which could arise as a consequence of weak spin-lattice interaction.

## 2. Experimental procedure

Conventional sol-gel method was used for obtaining nanoscale layered  $\text{SmFe}_{0.5}\text{Co}_{0.5}\text{O}_3$  perovskite sample [18]. The desired quantities of metal nitrates together with citric acid were dissolved in distilled water. The quantity of citric acid added to the solution was in the molar ratio of 1:2. The stirring of compound mixtures was done at 60 °C for 3 h and then the mixture was left undisturbed at 100 °C for gel formation to occur, which is then dried at 150 °C for 12 h. The obtained powdered compound was allowed to decompose in air at 250 °C for 24 h. The decomposed powder was sintered at various temperatures ranging 400 °C to 800 °C for few times with intermediate grinding. The resulting polycrystalline powder was ground again thoroughly and pressed into pellets, which were finally sintered in air at 950 °C for 48 h. The sintered pellets broken into small pieces were used for various measurements and ground again to form fine powder for recording X-ray diffraction with  $2\theta$  ranging from 10°-100°. The oxygen stoichiometry of the sample is checked by iodometric titration, which confirms the value of “ $\text{SmFe}_{0.5}\text{Co}_{0.5}\text{O}_3$ ” within the accuracy limit ( $3 \pm 0.05$ ). The sol-gel process allows the synthesis of single phase sample with uniform crystal morphologies at significantly lower temperature without any secondary phase, which are evidenced from transmission electron microscopy (TEM), HRTEM, electron diffraction (ED), HAAD-STEM and EELS studies [21]. Physical property measurement system (PPMS, Quantum Design) was used for investigating the field and temperature dependence of magnetization under different conditions. The dielectric investigations as a function of temperature and magnetic field were accomplished by using the PPMS coupled with an impedance analyser (Agilent technologies-4284A) in the temperature range of 10 K to 300 K, frequency range 10 kHz–500 kHz and applied magnetic field up to 14 Tesla. The applied electric and magnetic fields were in the same directions to eliminate the contribution due to

Hall-effect [22]. The electrodes on the pellets were prepared in capacitor geometry by painting with silver paste both sides of the polished pellets.

### 3. Results and discussion

The powder diffraction pattern of nanoscale layered  $\text{SmFe}_{0.5}\text{Co}_{0.5}\text{O}_3$  perovskite could be indexed with the orthorhombic symmetry in the space group of *Pnma* [21]. The X-ray diffraction pattern is presented in Fig. 1, whereas the refined data and lattice parameters are given in Table 1. Temperature dependent zero field cooled (ZFC) and field cooled (FC) magnetization for nanoscale layered  $\text{SmFe}_{0.5}\text{Co}_{0.5}\text{O}_3$  perovskite under the applied fields of 50, 200 and 1000 Oe with standard measurement protocol are shown in Fig. 2. The ZFC-FC magnetization,  $M(T)$ , increases with decrease in temperature and there is a sharp magnetic transition around 310 K. The FC data increases rapidly till 210 K, where a sudden change in slope (a kink) of  $M(T)$  curve occurs and thereafter, the value of magnetization decreases gradually up to 170 K. However, on further cooling the  $M(T)$  value increases and exhibits a broad maxima around 70 K. Finally, below 40 K the magnetization abruptly decreases to a lower value. Nevertheless, the 50 Oe ZFC data exhibit contrasting behaviours in the measured temperature range compared to higher applied fields. There is a large divergence between ZFC-FC in lower field (Fig. 2a) whereas the high field ZFC superimpose with FC data at higher applied fields (Fig. 2b & c). This complicated magnetic behavior below room temperature could be due to the two inequivalent magnetic sublattices; the 4f electron based Ln sublattice and 3d electron based Fe-Co sublattice, which are arranged antiparallely [17]. The 50 Oe ZFC magnetization curve demonstrates an antiferromagnetic ordering at 310 K ( $T_N$ ) and then occurs a spin-reorientation transition at 210 K ( $T_{SR1}$ ). Further lowering the temperatures, the system changes magnetization from negative to a positive value with a second spin-

reorientation at 22 K ( $T_{SR2}$ ). In contrast the 50 Oe FC data (Fig. 2a) show weak spin-reorientations transition below  $T_N$ , which diverge at 275 K and exhibits similar to the high field  $M(T)$  behavior. In the 50 Oe ZFC case, the spin-reorientations with the variation of temperature could be explained by the fact that the effective moment of Sm sublattice rotates and align in opposite directions to the Fe-Co sublattice, resulting in negative magnetization value. In the case of orthoferrites perovskite these two sublattices generally ordered magnetically at different temperatures as a result spin-reorientation phenomenon observed due to strong competition between the two magnetic sublattices. This type of magnetization reversal has been reported recently for  $ErFe_{0.5}Co_{0.5}O_3$  phase by Lohr et al [17]. The Ln sublattice ordered antiferromagnetically at relatively low temperatures, whereas transition metals ordering temperature is higher [10-12, 17]. Noteworthy, these magnetic transitions could be at the origin of resultant magnetization owing to strong coupling between 3d and 4f electrons from the Fe-Co and Ln sublattices. Therefore, the magnetic kink at 210 K and abrupt decrease in the  $M(T)$  value below 40 K could be due to the spin-reorientation.

Fig. 3 demonstrates the field dependent magnetization behaviour  $M(H)$  at 2, 100 and 350 K for nanoscale layered  $SmFe_{0.5}Co_{0.5}O_3$  to understand the type of magnetic interactions. The measurements are performed after zero field cooling the sample from room temperature to the desired temperature and then performing a full hysteresis loop (including the virgin curve). The system depicts hysteresis loop with large values of remnant magnetization (0.012  $\mu_B/f.u.$ ) and coercive field (6 kOe) at 100 K. Importantly, the magnetization value does not indicate any saturation even when the applied field strength is 5 Tesla, but the value increases almost linearly with the applied field and maximum value of magnetization is only 0.066  $\mu_B/f.u.$ , which is akin to the parent  $SmFeO_3$  perovskite [12]. The  $M(H)$  behaviour at 2 K is similar to that at 100 K, however, the corresponding values are lower (0.005  $\mu_B/f.u.$  & 2 kOe) in contrast to the expected values for magnetic perovskites. This could be due to the large

domain wall pinning of the magnetic spins at 100 K. Finally, at 350 K, the M(H) data depicts a linear behavior analogous to paramagnetic system. Hence, the behaviour of magnetic hysteresis loops below  $T_N$  clearly indicate that nanoscale layered  $\text{SmFe}_{0.5}\text{Co}_{0.5}\text{O}_3$  behaves as a canted antiferromagnet, in which due to canting of magnetic spins a weak ferromagnetism remains. The magnetic ordering at 310 K could be due to the canted nature of the magnetic spins, which are antiferromagnetically aligned [23]. This is well known for orthoferrites where the weak ferromagnetism is due to non-collinear antiferromagnetism in the Fe sublattice at higher temperature [11-17]. The weak ferromagnetism in these orthoferrites could also arise due to the asymmetric exchange or Dzyaloshinskii-Moriya interaction which results in canted antiferromagnetic order implying that the nonlinear motions of each sublattice spin along the direction of net magnetization do not cancel perfectly [17, 24]. This type of interaction has been well established for perovskite orthoferrites [10-20, 23, 24].

To investigate the magneto-dielectric correlation, we have studied temperature and magnetic field dependence of dielectric constant as well as dielectric loss for nanoscale layered  $\text{SmFe}_{0.5}\text{Co}_{0.5}\text{O}_3$  perovskite at various frequencies. Fig. 4 exhibits the temperature dependence of the real part of dielectric constant ( $\epsilon'$ ) and dielectric loss ( $\tan\delta$ ), examined at various frequencies. The  $\epsilon'$  value increases with increasing temperature with a rapid jump around 100 K, with further increase in temperature the sample does not show any maximum in  $\epsilon'$  as usually noticed for conventional dielectrics and the  $\epsilon'$  value increases continuously with increasing temperature. This type of behavior can be explained by dipolar type relaxation coupled with variable type hopping conduction of the charge carrier, which is a familiar phenomenon in case of semiconductors [22, 25, 26]. The localized charge carrier usually hops between spatially fluctuating lattice potentials, which produce conductivity as well as dipolar effect. This type of dielectric behavior has been reported for polycrystalline

Fe-doped perovskite [26]. Noteworthy, the magnitude of the dielectric constant of this perovskite system decreases with increase in frequency which indicates that the present nanoscale layered  $\text{SmFe}_{0.5}\text{Co}_{0.5}\text{O}_3$  perovskite exemplifies a relaxor-like behavior. Prominent  $\tan\delta$  peaks (Fig. 4b) are observed in the region where dielectric constant rapidly changes its behaviour. Shifting of  $\tan\delta$  peaks towards higher temperature with increase in frequency indicates a thermally activated relaxation. Due to the presence of dc conductivity in this perovskite (semiconducting type) the  $\tan\delta$  increases with temperature i.e. near the room temperature the loss ( $\tan\delta$ ) is doubled compared to the peak value (Fig. 4b).

From the previous studies it is clear that, the magnetic and dielectric transitions appear below room temperature, which could provide some correlation between magnetic and dielectric properties. Hence, isothermal magneto-dielectric studies have been carried out at different temperatures. Fig. 5(a) exhibits the magnetic field dependent dielectric constant for nanoscale layered  $\text{SmFe}_{0.5}\text{Co}_{0.5}\text{O}_3$  perovskite at four different temperatures and at higher frequency 100 kHz [22]. A positive magneto-dielectric value of 2.5% is obtained at 100 K, which is calculated as  $\Delta\epsilon = [(\epsilon_H - \epsilon_0)/\epsilon_0] \times 100$ , where  $\epsilon_H$  and  $\epsilon_0$  are the dielectric constant values in presence and absence of magnetic fields [22, 25]. Above and below this temperature the value is significantly smaller, although magneto-dielectric coupling is prominent above 100 K. So, for further understanding of the origin of this behaviour observed at high temperatures, temperature dependent dielectric investigations in the presence and absence of magnetic field are carried out. Figs. 5(b) and (c) show the temperature dependent  $\epsilon'$  and loss ( $\tan\delta$ ) of the system at different magnetic fields (frequency at 100 kHz). The dielectric constant value varies from 10 to 170 in the temperature range 10-300 K. At low temperature ( $< 90$  K) the dielectric constant values are independent of frequency and temperature. Around 100 K, a sudden increase of dielectric constant value is observed. The rapid increase of dielectric constant values above 100 K could arise due to numerous factors which may be e.g.

intrinsic and/or extrinsic to the system [22, 25-30] and we have analysed the data in details to confirm the actual effect. The rapid increase of  $\epsilon'$  value within small interval of temperature may arise due to onset of ferroelectric ordering in which the dipoles are subjected to a double well energy barrier [29]. This effect is intrinsic to the system and the  $\epsilon'$  value follows Curie-Weiss behavior beyond the ferroelectric ordering. However, for nanoscale layered  $\text{SmFe}_{0.5}\text{Co}_{0.5}\text{O}_3$  perovskite, we do not observe any peak in the  $\epsilon'$  value. Hence, a combined effect of the grain boundary and the space charge effect may be responsible for the observed behaviour above 100 K. This arises due to semiconducting nature of the nanoscale layered  $\text{SmFe}_{0.5}\text{Co}_{0.5}\text{O}_3$  perovskite associated with the contact effects. In contrast, the low temperature magneto-dielectric coupling is solely due to the intrinsic spin-lattice interaction, which give rise to a positive magneto-capacitance effect with a maximum value around 100 K. It is worth mentioning that, the positive value of magneto-dielectric constant is reported to be originated from the spin-lattice interaction, which is an intrinsic property of the system [22, 25, 30]. Additionally, the magnetic field dependent dielectric loss ( $\tan\delta$ ) at 100 kHz (inset Fig. 5c) exhibits similar trend of shift to the  $\epsilon'$  value as expected for intrinsic magneto-dielectric effect [22].

#### 4. Conclusions

This work presents the low temperature magnetic and dielectric as well as magneto-dielectric coupling of mixed iron-cobalt based nanoscale layered  $\text{SmFe}_{0.5}\text{Co}_{0.5}\text{O}_3$  perovskite. The complex nature of magnetic behavior is reflected from multiple transitions in the low temperature regions. Such complex behaviour can be ascribed to the different ordering temperatures of the magnetic sublattices and interaction between the 3d and 4f sublattices. The magnetic interactions are prevalently antiferromagnetic in nature. However, the antisymmetric or Dzyaloshinskii-Moriya interaction may be considered as the genesis of

weak ferromagnetism in the nanoscale layered  $\text{SmFe}_{0.5}\text{Co}_{0.5}\text{O}_3$ . The dielectric measurements reveal the relaxor-like behaviour at low temperature. More importantly, we observed an intrinsic magneto-dielectric effect  $\sim 2.5\%$  around 100 K. This result suggests the active coupling between the ordering in magnetic and electric parameters which is of paramount importance from the view point of next generation magneto-electric devices. We hope this result will pave the way to explore the material with large magneto-dielectric coupling at room temperature.

### **Acknowledgements**

The authors would like to thank the Science and Engineering Research Board (IN), India for financial support through the project grant # EMR/2016/000083 and Prof. B. Raveau for his valuable comments and suggestions.

### **References:**

- [1] A.V. Kimel, A. Kirilyuk, P.A Usachev, R.V Pisarev, A.M Balbashov, Th. Rasing, *Nat.* 435 (2005) 655-657.
- [2] M. Fiebig, *J. Phys. D* 38 (2005) R123-R152.
- [3] W. Eerenstein, M. Wiora, J. L. Prieto, J. F. Scott, N. D. Mathur, *Nat. Mater.* 6 (2007) 348-351.
- [4] Y. Tokunaga, S. Iguchi, T. Arima, Y. Tokura, *Phys. Rev. Lett.* 101 (2008) 097205.
- [5] Y. Tokunaga, N. Furukawa, H. Sakai, Y. Taguchi, T. Arima, Y. Tokura, *Nat. Mater.* 8 (2009) 558-562.
- [6] R.V. Mikhaylovskiy, E. Hendry, A. Secchi, J.H. Mentink, M. Eckstein, A. Wu, R.V. Pisarev, V.V. Kruglyak, M.I. Katsnelson, Th. Rasing, A.V. Kimel, *Nat. Commun.* 6 (2015) 8190.
- [7] R. V. Mikhaylovskiy, T. J. Huisman, R. V. Pisarev, Th. Rasing, A. V. Kimel, *Phys. Rev. Lett.* 118 (2017) 017205.
- [8] J.A. de Jong, A.V. Kimel, R.V. Pisarev, A. Kirilyuk, Th. Rasing, *Phys. Rev. B* 84 (2011) 104421.

[9] T. F. Nova, A. Cartella, A. Cantaluppi, M. Först, D. Bossini, R. V. Mikhaylovskiy, A. V. Kimel, R. Merlin, A. Cavalleri, *Nat. Phys.* 13 (2017) 132-136.

[10] X. Li, M. Bamba, N. Yuan, Q. Zhang, Y. Zhao, M. Xiang, K. Xu, Z. Jin, W. Ren, G. Ma, S. Cao, D. Turchinovich, J. Kono, *Science* 361 (2018) 794–797.

[11] S.J. Yuan, W. Ren, F. Hong, Y.B. Wang, J.C. Zhang, L. Bellaiche, S.X. Cao, G. Cao, *Phys. Rev. B* 87 (2013) 184405.

[12] J.H. Lee, Y. K. Jeong, J. H. Park, M.-A. Oak, H. M. Jang, J. Y. Son, J. F. Scott, *Phys. Rev. Lett.* 107 (2011) 117201.

[13] R. D. Johnson, N. Terada, P. G. Radaelli, *Phys. Rev. Lett.* 108 (2012) 219701.

[14] J.H. Lee, Y. K. Jeong, J. H. Park, M.-A. Oak, H. M. Jang, J. Y. Son, J. F. Scott, *Phys. Rev. Lett.* 108 (2012) 219702.

[15] C.Y. Kuo, Y. Drees, M. T. Fernández-Díaz, L. Zhao, L. Vasylechko, D. Sheptyakov, A. M. T. Bell, T. W. Pi, H.-J. Lin, M.-K. Wu, E. Pellegrin, S. M. Valvidares, Z. W. Li, P. Adler, A. Todorova, R. Küchler, A. Steppke, L. H. Tjeng, Z. Hu, A. C. Komarek, *Phys. Rev. Lett.* 113 (2014) 217203.

[16] G. Kotnana, S. N. Jammalamadaka, *J. Mag. Mag. Mater.* 418 (2016) 81-85.

[17] J. Lohr, F. Pomiro, V. Pomjakushin, J. A. Alonso, R. E. Carbonio, R. D. Sánchez, *Phys. Rev. B* 98 (2018) 134405.

[18] V. Solanki, S. Das, S. Kumar, M. M. Seikh, B. Raveau, A. K. Kundu, *J. Sol-Gel Sci. Technol.* 82 (2017) 536.

[19] N. B. Ivanova, N. V. Kazak, C. R. Michel, A. D. Balaev, S. G. Ovchinnikov, *Physics of the Solid State* 49 (2007) 2126-2131.

[20] M. Tachibana, T. Yoshida, H. Kawaji, T. Atake, E. T. Muromachi, *Phys. Rev. B* 77 (2008) 094402.

[21] N. E. Mordvinova, A. Shukla, A. K. Kundu, O. I. Lebedev, M. M. Seikh, V. Caignaert, B. Raveau, arxiv (<http://arxiv.org/abs/1811.05221>).

[22] H. M. Rai, S. K. Saxena, V. Mishra, R. Kumar, P. R. Sagdeo, *J. App. Phys.*, 122, (2017) 054103.

[23] D. V. Karpinsky, I. O. Troyanchuk, V. V. Sikolenko, *J. Phys.: Condens. Matter* 17 (2005) 7219.

[24] J. Lu, X. Li, H. Y. Hwang, B. K. Ofori-Okai, T. Kurihara, T. Suemoto, K. A. Nelson, *Phys. Rev. Lett.*, 118 (2017) 207204

[25] G. Catalan, *Appl. Phys. Lett.*, 88 (2006) 102902.

[26] A. K. Kundu, V. K. Jha, M. M. Seikh, R. Chatterjee, R. Mahendirian, *J. Phys.: Condens. Matter* 24 (2012) 255902.

[27] T. Moriya, Phys. Rev. Lett. 4 (1960) 228.

[28] L. E. Cross, Ferroelectrics 76 (1987) 241-267.

[29] P. Lunkenheimer, V. Bobnar, A. V. Pronin, A. I. Ritus, A. A. Volkov, A. Loidl, Phys. Rev. B 66 (2002) 052105.

[30] A. K. Kundu, R. Ranjith, V. Pralong, V. Caignaert, B. Raveau, J. Mater. Chem., 18 (2008) 4280-4285.

**Table. 1.** Lattice parameters of nanoscale layered  $\text{SmFe}_{0.5}\text{Co}_{0.5}\text{O}_3$  perovskites. Here  $a$ ,  $b$ ,  $c$  are the lattice parameters,  $R_b$  and  $R_f$  are the Bragg factor and fit factor, respectively.

Perovskite	$\text{SmFe}_{0.5}\text{Co}_{0.5}\text{O}_3$
Space group	$Pnma$
$a$ (Å)	5.484(6)
$b$ (Å)	7.611(3)
$c$ (Å)	5.348(4)
$V$ (Å <sup>3</sup> )	223.410
$\alpha, \beta, \gamma$	90°, 90°, 90°
Bond length	Sm—O1 : 2.305 Å Sm—O1 : 2.444 Å Sm—O2 : 2.444 Å Sm—O2 : 2.305 Å Fe/Co—O1 : 1.968 Å Fe/Co—O1: 1.972 Å Fe/Co—O2 : 1.974 Å
Bond angle	<Fe/Co—O1—Fe/Co>: 159.7° <Fe/Co—O2—Fe/Co>: 157.3°
$R_b$ (%)	11.3
$R_f$ (%)	19.9
$\chi$ -factor	2.87

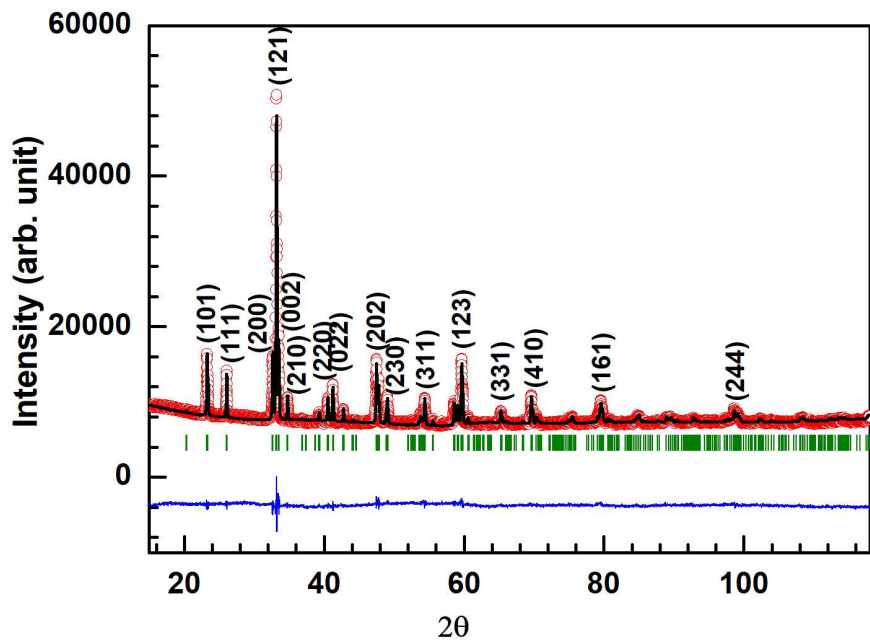


**Fig. 1.** Rietveld analysis of XRD pattern for nanoscale layered  $\text{SmFe}_{0.5}\text{Co}_{0.5}\text{O}_3$ . Open symbols are experimental data and the solid and vertical lines represent the difference curve and Bragg positions respectively.

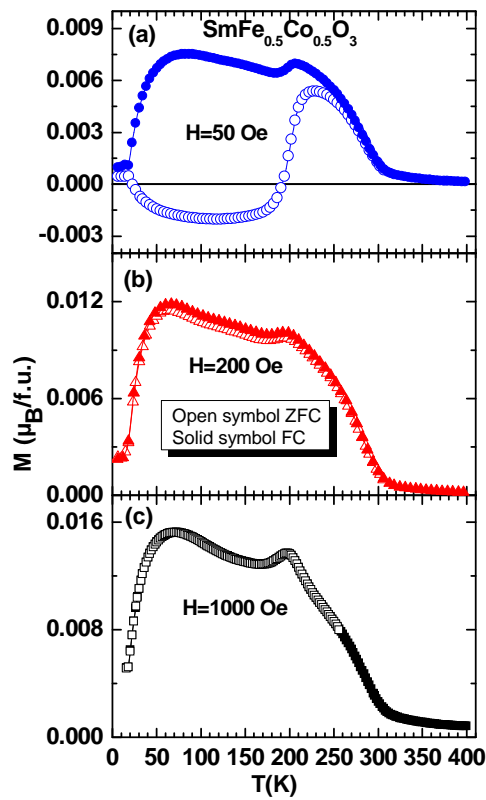


**Fig. 2** Temperature dependent ZFC (open symbol) and FC (solid symbol) magnetization,  $M$ , for nanoscale layered  $\text{SmFe}_{0.5}\text{Co}_{0.5}\text{O}_3$  under the fields of (a)  $H=50$  Oe, (b)  $H=200$  Oe and (c)  $H=1000$  Oe.

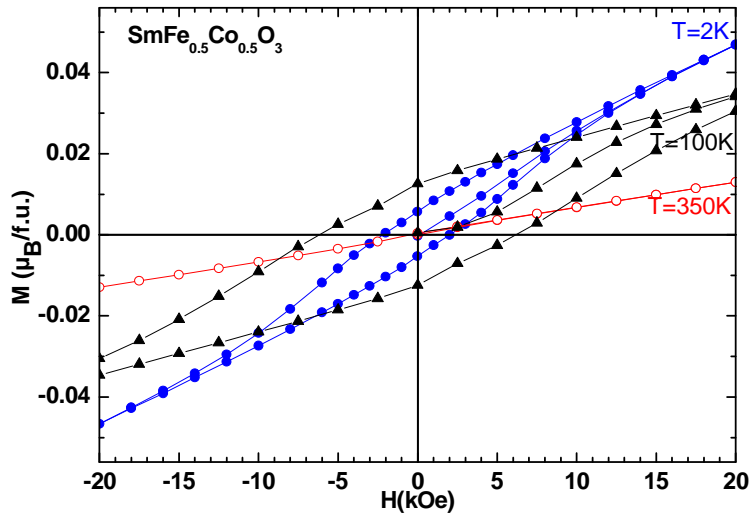


**Fig. 3** Field dependent isothermal magnetic hysteresis,  $M(H)$ , curves at three different temperatures for nanoscale layered  $\text{SmFe}_{0.5}\text{Co}_{0.5}\text{O}_3$ .

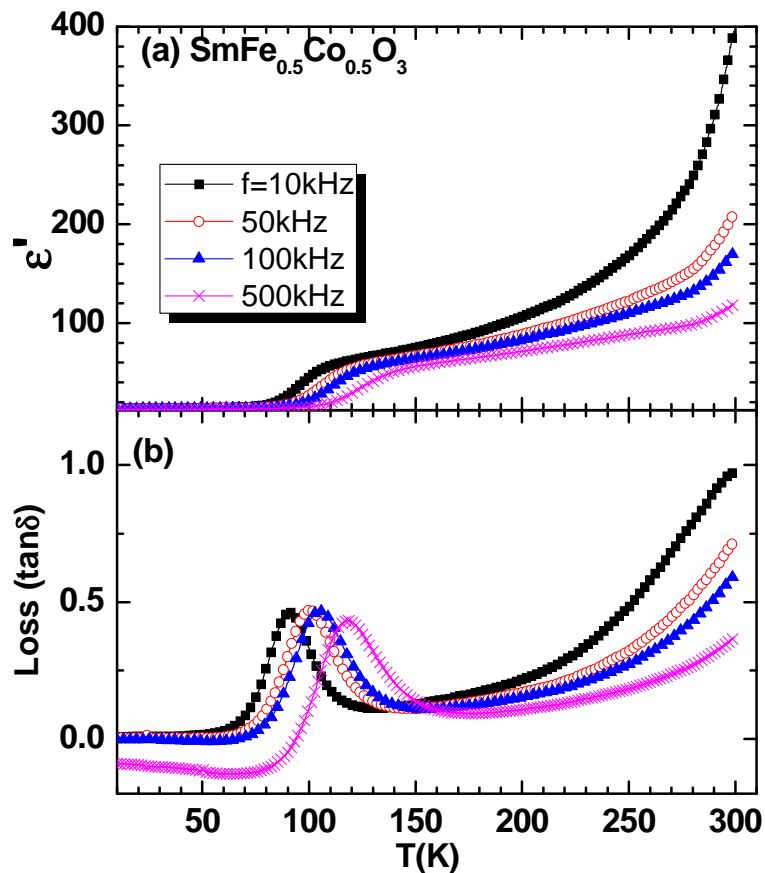


**Fig. 4** Temperature dependent (a) dielectric constant and (b) dielectric loss for nanoscale layered  $\text{SmFe}_{0.5}\text{Co}_{0.5}\text{O}_3$  at different frequencies.

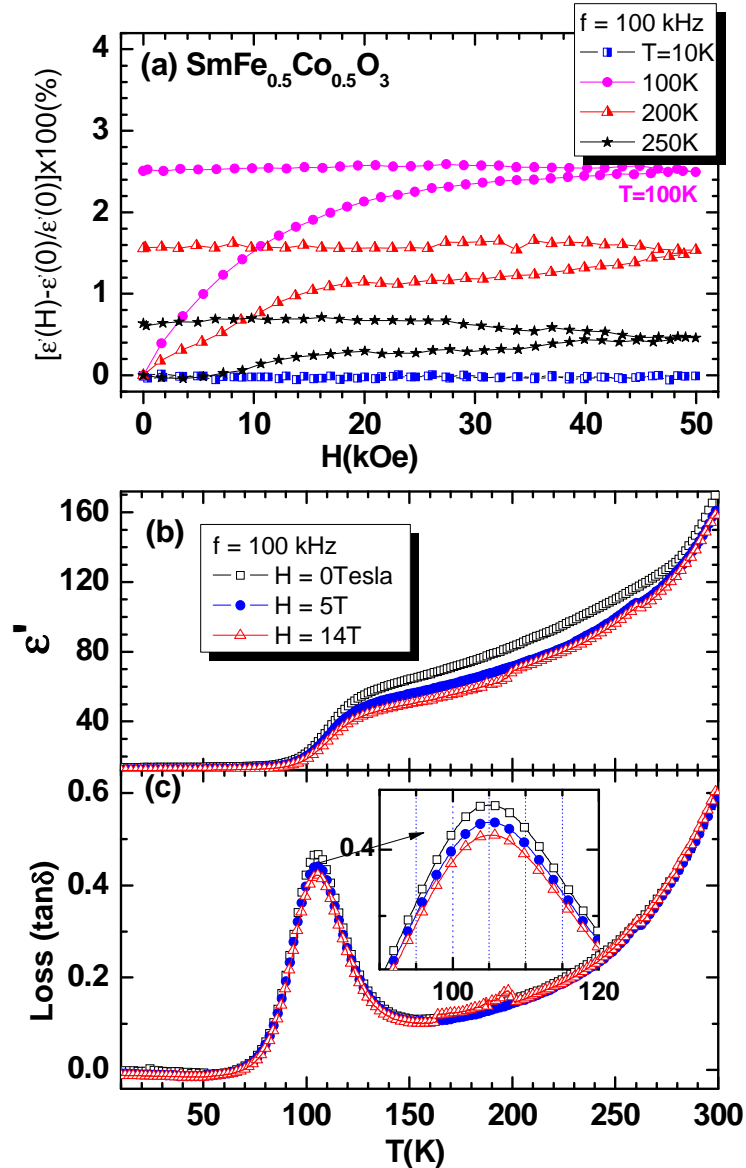


**Fig. 5** (a) Field dependent isothermal dielectric constant at four different temperatures and (b-c) temperature dependent dielectric constant and loss in three different fields for nanoscale layered  $\text{SmFe}_{0.5}\text{Co}_{0.5}\text{O}_3$ . Inset figure shows the magnified dielectric loss peak.